

# Identification of effective stimulation parameters to abort epileptic seizures in a neural mass model

Marouan Arrais, Fabrice Wendling, Julien Modolo

**Abstract**— Pathological brain activity can be modulated by using electrical stimulation. However, one major challenge is the identification of the optimal parameter values normalizing pathological activity towards more physiological patterns. One possible approach to address this challenge is the use of computational models. Here, we used a validated neural mass model (NMM) to simulate epileptiform activity and its modulation by electrical stimulation. Based on simple features of the simulated signals before and during stimulation within the time and frequency domains, we studied the effectiveness of a given stimulation parameters. Stimulations inducing a membrane polarization greater than 4 mV and a frequency over 25 Hz were identified as common effective parameters for the majority of epileptiform signals. This work provides further evidence for model-guided stimulation parameters optimization as a rationale for neuromodulation therapy refinement.

## I. INTRODUCTION

Brain stimulation is an effective method to modulate neural activity and treat several brain diseases, such as epilepsy [1], [2]. The stimulation parameters such as amplitude, frequency and waveform play a critical role in therapeutic effects such as seizure abortion in epilepsy. Stimulation parameters can indeed result either in effective seizure abortion, or in exacerbation of epileptiform activity. Therefore, identifying the optimal parameter set within an immense parameter space is especially challenging.

Significant research efforts have been made over the last decades to identify effective stimulation parameters in specific therapeutic applications. Some studies have argued for the efficacy of high stimulation frequencies (typically at 100 Hz) [3]–[5], while others provided evidence low frequency stimulation (frequency lower than 5 Hz) as an effective perturbation able to reduce seizures frequency [6], [7]. A common conclusion from those studies is that the most effective stimulation parameters remains unknown to date. Here, we investigate seizure abortion within a neural mass model as a function of two stimulation parameters: stimulation amplitude and frequency, as an attempt to identify optimal stimulation parameters.

## II. METHODS

We aimed at identifying stimulation parameters resulting in the replacement of epileptic activity by a more physiological one through the use of a neural mass model (NMM). First, we introduce the NMM and the type of stimulation used. Second, we present our method to

Research supported by the National Institutes of Health (NIH), grant number: R01 NS092760-01A1.

M. Arrais, F. Wendling, J. Modolo are with the university of Rennes 1, INSERM, LTSI – U1099, F-35000 Rennes, France (e-mail: [marouan.arrais@etudiant.univ-rennes1.fr](mailto:marouan.arrais@etudiant.univ-rennes1.fr), [fabrice.wendling@inserm.fr](mailto:fabrice.wendling@inserm.fr), [julien.modolo@inserm.fr](mailto:julien.modolo@inserm.fr)).

quantitatively evaluate the effectiveness of stimulation parameters.

### A. Wendling's neural mass model

One of the most frequently used neural mass models (NMM) is Wendling's model [8], an extension of the well-known Jansen and Rit model [9] producing a large variety of EEG (electroencephalographic) signals and rhythms. Wendling's model provides realistic markers of epileptiform activity such as high-frequency oscillations (HFOs) and low-frequency rhythmic spikes (4-6 Hz).

Wendling's model involves three neural populations (Fig. 1), each involving two operators as in Jansen and Rit's model. The first operator  $h_k(t)$  converts the average firing rate describing the input to a population into an average excitatory or inhibitory postsynaptic membrane potential [10], with the response function given by:

$$h_k(t) = A_k a_k t e^{-a_k t} \quad (1)$$

where  $A_k$  represents the average excitatory or inhibitory synaptic gain, and  $a_k$  represents the average time constant of post synaptic potentials. This operator can also be described as a linear second-order ordinary equation:

$$\ddot{y} = A_k a_k x - 2a_k \dot{y} - a_k^2 y \quad (2)$$

where  $x, y$  are the input and output signals, respectively.

The second operator  $Sig$  converts the population average membrane potential into its mean firing activity through a sigmoidal transformation:

$$Sig(v) = \frac{2e_0}{1+e^{r(v_0-v)}} \quad (3)$$

where  $e_0$  is the mean firing rate of the neurons,  $v_0$  is the value of the potential corresponding to the inflection point of the sigmoid (activity threshold of the population) and  $r$  is the slope of the sigmoid at  $v_0$ . The summation of the membrane potential on pyramidal cells represents the EEG signal.

### B. Brain stimulation

Despite the fact that the stimulation waveform is typically represented by a train of pulses with specific parameters (amplitude, frequency and pulse width) [3], [11], in the following we applied a sinusoidal stimulation  $S$ . The advantage is that this waveform involves a unique frequency component, rather than multiple ones as for biphasic pulses. Hence, we will identify which exact frequency is the most effective to modulate the activity of a neural population.

Stimulation was applied on each neural subpopulation, more specifically before each sigmoid function to account for an effect on the membrane potential. Therefore, the model is described by 5 2nd-order ordinary differential equations; one equation for each neural population, plus the inhibitory

synaptic projection between slow and fast inhibitory interneurons:

$$\begin{aligned}\ddot{y}_0(t) &= Aa\text{Sig}(S + y_1 - y_2 - y_3) - 2a\dot{y}_0(t) - a^2y_0(t) \\ \dot{y}_1(t) &= Aa\{p(t) + \text{Sig}(S + C_1y_0)\} - 2a\dot{y}_1(t) - a^2y_1(t) \\ \dot{y}_2(t) &= BbC_4\text{Sig}(S + C_3y_0) - 2b\dot{y}_2(t) - b^2y_2(t) \\ \dot{y}_3(t) &= GgC_7\text{Sig}(S + C_5y_0 - y_4) - 2g\dot{y}_3(t) - g^2y_3(t) \\ \dot{y}_4(t) &= BbC_6\text{Sig}(S + C_3y_0) - 2b\dot{y}_4(t) - b^2y_4(t)\end{aligned}\quad (4)$$

where  $p(t)$  depicts a Gaussian noise of mean and standard deviation equal to 90 and 30 (expressed in pulses per second), respectively. Other model parameters and their interpretation are provided in Table I.

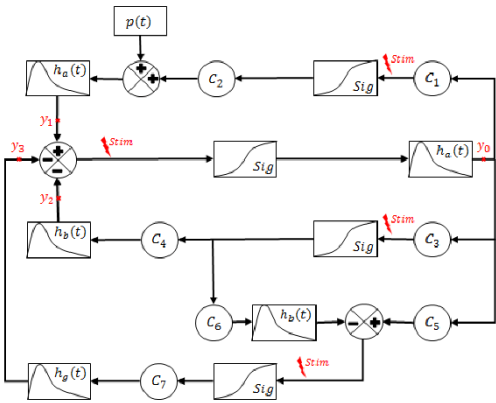


Fig. 1. Block diagram of Wendling's NMM.  $y_i, i \in \{0, 1, 2, 3\}$  correspond to the output of pyramidal cells, excitatory and both slow and fast inhibitory interneurons, respectively. The red flash symbol represents the stimulation position.

TABLE I: PARAMETERS USED IN WENDLING'S NEURAL MASS MODEL

Parameter	Description	Values
$A, B, G$	Average gains of excitatory, slow and fast inhibitory synaptic gains, respectively.	$A \in [0.1, 10 \text{ mV}]$ $B \in [0.1, 50 \text{ mV}]$ $G \in [20, 50 \text{ mV}]$
$a, b, g$	Average time constants of post-synaptic potentials.	$a = 100 \text{ s}^{-1}$ $b = 30 \text{ s}^{-1}$ $g = 350 \text{ s}^{-1}$
$C_1, C_2, C_3, C_4, C_5, C_6, C_7$	Average number of synaptic contacts of excitatory and inhibitory connections.	$C_1 = J$ $C_2 = C_7 = 0.8 \times J$ $C_3 = C_4 = 0.25 \times J$ $C_5 = 0.3 \times J$ $C_6 = 0.1 \times J$ Where $J = 135$ .

### C. Classification of signals generated by Wendling's NMM

Wendling's model enables simulating five different rhythms (background, spikes, slow rhythmic, alpha and fast activity), as presented in Fig. 2. In this study, we focused on slow rhythmic activity. At the onset of seizures, EEG is indeed characterized by a mixing of rhythmic spikes and slow rhythmic activity. Later on, spikes disappear, and slow rhythmic activity lasts 10 to 15 s before that a low-amplitude rapid discharge of a frequency typically beyond over 25 Hz is observed. Since we aimed at studying how to abort epilepsy seizures at their onset, our goal was to identify effective stimulation parameters able to suppress slow

rhythmic oscillations and replace them by a physiological "background" activity. Therefore, we started by classifying the signals generated by the model without stimulation into three groups: background, slow rhythmic and others. Slow rhythmic activity is known by a dominant frequency inferior to 8 Hz, therefore, all triplets (A, B, G) that generate signals of a dominant frequency greater than 8 Hz (alpha and fast activity) were rejected and not retained for further analysis. The remaining triplets could generate slow rhythmic activity, but also spikes and background. To distinguish between these rhythms, the magnitude of the dominant frequency and number of peaks were analyzed. Signals with a dominant frequency magnitude inferior to 0.1 mV<sup>2</sup>/Hz were considered as background. This threshold was defined based on a study of background signals. Moreover, to discriminate spikes from rhythmic activity, we conducted a peak detection on a 10 s portion of the EEG generated by the remaining triplets. All epochs with less than 10 peaks were considered as spikes.

As a result, we obtained all the triplets (A, B, G) that generate slow rhythmic and background signals of specific power spectrum, maximum and minimum values.

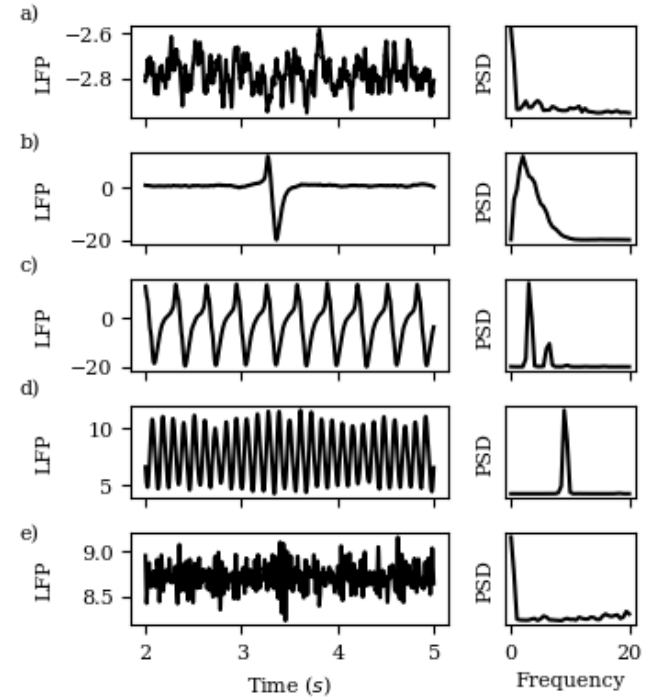


Fig. 2. EEG patterns generated by Wendling's NMM and their frequency spectrum. To generate these signals, the fast inhibitory synaptic gain was fixed at 20 mV, while excitatory and slow inhibitory synaptic gains had the following values: a) background activity: (A,B)=(2,24), b) spikes: (A,B)=(5, 23), c) slow rhythmic activity: (A,B)=(5.5, 20), d) alpha rhythm: (A,B)=(6,9) and e) fast activity: (A,B)=(5,1).

### D. Effectiveness of stimulation parameters

Model synaptic gains were fixed to generate a slow rhythmic activity. The effectiveness of a given stimulation parameters (amplitude, frequency) was quantified based on a comparison of both the root mean square (RMS) of the power spectrum and the difference between maximum and minimum values of signals before and during stimulation. If the signal obtained after stimulation had a peak-to-peak

value inferior than or equal to 10 % as compared to the original signal without stimulation; and simultaneously, a power spectrum RMS on the interval [0, 8] Hz inferior or equal to 0.005 % of the original signal without stimulation, stimulation settings were considered as effective. These thresholds were fixed based on the signals in “background activity” mode, based a comparison of background and slow rhythmic signals determined after classification of signals generated by Wendling’s NMM without stimulation. For example, the maximum RMS of the power spectrum on the interval [0, 8 Hz] of rhythmic activities was equal to 199.24, and 0.01 for background. Hence, the second value represents 0.005 % of the first one.

#### E. Optimal stimulation parameters

For each rhythmic configuration of triplet (A, B, G), we applied a sinusoidal stimulation frequency between 1 Hz and 120 Hz, with a step of 1 Hz and an amplitude between 1 mV and 5 mV with a step of 0.2. For all EEGs obtained during stimulation, we studied the power spectrum, maximum and minimum values. Therefore, we obtained EEGs generated without stimulation and another 2380 EEGs generated by using all possible stimulation settings. Then, the comparison process of the power spectrum RMS on the interval [0, 8 Hz] and the difference between the maximum and minimum values was performed. As a result, for each stimulation setting, we obtained the number of triplets (A, B, G) for which this stimulation was considered effective. By dividing this number by the number of all triplets generating a rhythmic activity, we obtained an index to classify the stimulation and determined which one is effective for the majority of slow rhythmic activities. The corresponding results are presented in section III.C.

### III. RESULTS

In this section, the effectiveness of a set of stimulation parameters to impact a particular rhythmic activity is studied. Then, stimulation parameters able to impact the majority of rhythmic activities generated by the model are presented.

#### A. Effective versus non-effective stimulation parameters for a particular rhythmic activity

The model output was set in rhythmic activity, synaptic gains were fixed at 5.5 mV for the average excitatory synaptic gain, 25 mV for the slow inhibitory synaptic gain, and 20 mV for the fast inhibitory synaptic gain. Depending on the stimulation frequency, qualitatively different EEG patterns were obtained during stimulation, as illustrated in Figure 3.

A stimulation with an amplitude of 3 mV and a frequency of 90 Hz was identified as effective, and results in the replacement of the rhythmic activity presented in Fig. 3a by the activity pattern presented in Fig. 3b, having a power spectrum comparable to background activity. At the opposite, a stimulation with an amplitude of 4 mV and a frequency of 5 Hz was identified as non-effective, which was confirmed by the LFP time series during stimulation and its power spectrum. This result motived the systematic identification of effective settings for this particular rhythmic configuration within the (amplitude, frequency) - plane.

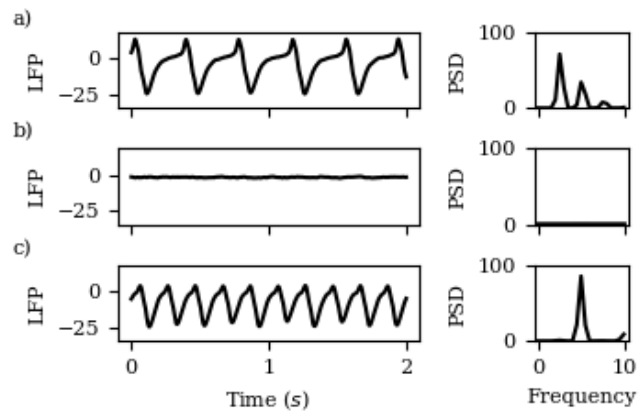


Fig. 3. Effective versus non-effective stimulation. a) Rhythmic activity generated for average synaptic gains equal to  $(A, B, G) = (5.5, 25, 20)$ . b) LFP obtained with an effective stimulation with an amplitude and frequency of 3 and 90 Hz, respectively. c) LFP obtained with a non-effective stimulation with an amplitude and frequency equal to 4 mV and 5 Hz, respectively.

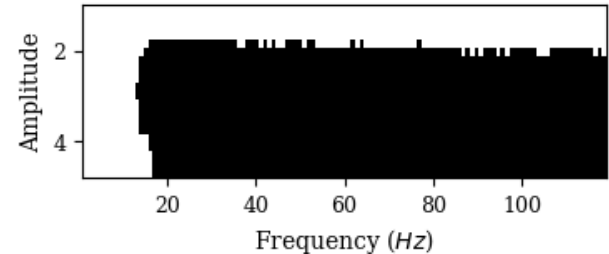


Fig. 4. Effective stimulation settings map. The black region represents effective stimulation parameters, while the white region represents non-effective ones. The average synaptic gains were adjusted to generate a rhythmic activity  $(A, B, G) = (5.5, 25, 20)$ .

Figure 4 illustrates the effectiveness of different stimulation settings. Stimulation settings such that the amplitude was greater than 2 mV and the frequency was greater than 18 Hz were identified as effective. Conversely, parameters below these threshold values were detected as non-effective. This result suggests that a wide range of stimulation settings could be used to replace rhythmic oscillations by a background activity.

#### B. Dependence of the effective stimulation parameters on the synaptic gains

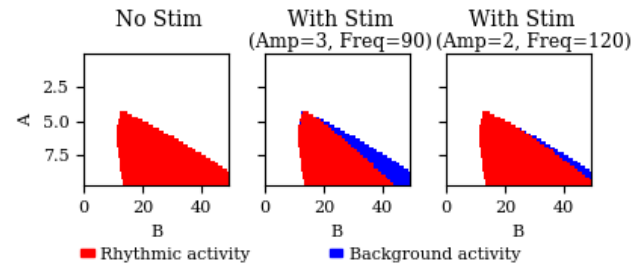


Fig. 5. Two-dimensional map of stimulation settings on epileptiform activity.

Let us note that a given set of stimulation parameters can be effective for multiple rhythmic activities. Figure 5 shows that a stimulation of an amplitude equal to 2 mV and a frequency equal to 120 Hz was able to replace a large number of rhythmic activities generated for the corresponding values of excitatory and slow inhibitory

synaptic gains by a background activity. However, the number of rhythmic EEGs (couples (A, B)) affected by this stimulation was much lower than those affected by a stimulation of amplitude equal to 3 mV and a frequency equal to 90 Hz.

Such a result motivates the search for stimulation parameters that are effective for the majority of rhythmic signals.

### C. Optimal stimulation parameters

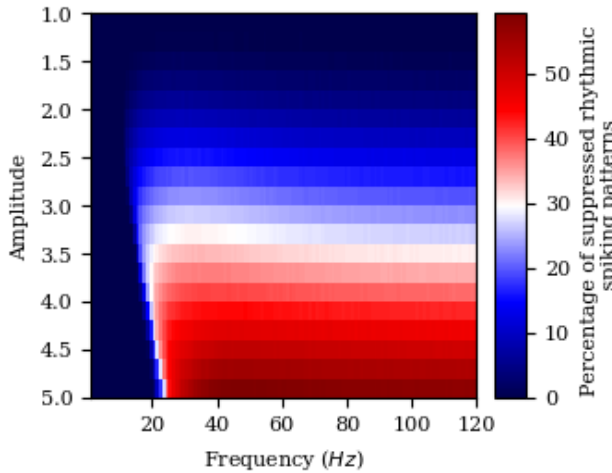


Fig. 6. Effectiveness of stimulation settings in epileptic seizures.

Figure 6 discriminates effective stimulation settings from non-effective ones, and points at the common effective stimulation settings. Actually, all sinusoidal stimulations with an amplitude lower than 2 mV and a frequency lower than 20 Hz were identified as non-effective, similarly as the result presented in Fig. 4. Moreover, sinusoidal stimulations with an amplitude greater than 4.5 mV and a frequency greater than 30 Hz were as effective for more than 35 % of rhythmic activities generated by the model. For example, a sinusoidal stimulation with an amplitude of 4.8 mV and a frequency of 45 Hz was effective in suppressing epileptiform activity for 60 % of the rhythmic activities generated.

The results presented in Fig. 6 were obtained after performing more than 21 million simulations on a computing cluster with 40 processors over a period of 57 hours.

### IV. DISCUSSION AND CONCLUSION

The Wendling's NMM was used to simulate brain activities. Based on simple time- and frequency- domains features, effective stimulation parameters (amplitude, frequency) were predicted within an immense parameter space. These effective parameters replaced epileptiform activity by a more physiological one. Unsurprisingly, both amplitude and frequency of stimulations were key to abort epileptiform activity. Stimulations of amplitude greater than 2 mV and frequency greater than 20 Hz were considered as effective, and conversely stimulations of frequency lower than 20 Hz were not able to abort the epileptic behavior.

Several couples (amplitude, frequency) replaced epileptiform activity by background activity; however, a stimulation of an amplitude equal to 5 mV and a frequency greater than 30 Hz was detected as an effective stimulation

for more than 30 % of rhythmic activities produced by Wendling's model.

These results support the previous works promoting the use of high-frequency stimulation; and also shed light on the influence of stimulation amplitude. As presented in Fig. 4, a stimulation of an amplitude lower than 2 mV was detected as non-effective whatever it is its frequency. These results illustrate that the effectiveness of stimulation to abolish epileptiform activity and replace it by a physiological pattern depends on the stimulation frequency when the stimulation amplitude belongs to the interval [2,5 mV]. Furthermore, if the stimulation amplitude is lower than 2 mV, the stimulation is non-effective irrespective of frequency.

Possible extensions of this work include the possibility to account for differential effects of brain stimulation on different neuronal types, which could be implemented in our model by adding a different stimulation-coupling coefficient for each neuronal type. Another possibility would be to increase the physiological realism of the coupling between the stimulation and neuronal populations, e.g. spatial distribution of the electric field or variable spatial orientation of neuronal types.

### ACKNOWLEDGMENT

This work is supported by the National Institutes of Health (NIH), grant number: R01 NS092760-01A1.

### REFERENCES

- [1] G. D. Wright and R. O. Weller, "Biopsy and post-mortem findings in a patient receiving cerebellar stimulation for epilepsy," *J. Neurol. Neurosurg. Psychiatry*, vol. 46, no. 3, pp. 266–273, Mar. 1983.
- [2] A. R. Upton and I. S. Cooper, "Some neurophysiological effects of cerebellar stimulation in man," *Can. J. Neurol. Sci. J. Can. Sci. Neurol.*, vol. 3, no. 4, pp. 237–254, Nov. 1976.
- [3] M. Filali, W. D. Hutchison, V. N. Palter, A. M. Lozano, and J. O. Dostrovsky, "Stimulation-induced inhibition of neuronal firing in human subthalamic nucleus," *Exp. Brain Res.*, vol. 156, no. 3, pp. 274–281, Jun. 2004.
- [4] K.-Z. Shen, Z.-T. Zhu, A. Munhall, and S. W. Johnson, "Synaptic plasticity in rat subthalamic nucleus induced by high-frequency stimulation," *Synap. N. Y. N.*, vol. 50, no. 4, pp. 314–319, Dec. 2003.
- [5] C. Beurrier, B. Bioulac, J. Audin, and C. Hammond, "High-frequency stimulation produces a transient blockade of voltage-gated currents in subthalamic neurons," *J. Neurophysiol.*, vol. 85, no. 4, pp. 1351–1356, Apr. 2001.
- [6] B. C. Albensi, G. Ata, E. Schmidt, J. D. Waterman, and D. Janigro, "Activation of long-term synaptic plasticity causes suppression of epileptiform activity in rat hippocampal slices," *Brain Res.*, vol. 998, no. 1, pp. 56–64, Feb. 2004.
- [7] K. Jerger and S. J. Schiff, "Periodic pacing an in vitro epileptic focus," *J. Neurophysiol.*, vol. 73, no. 2, pp. 876–879, Feb. 1995.
- [8] F. Wendling, F. Bartolomei, J. J. Bellanger, and P. Chauvel, "Epileptic fast activity can be explained by a model of impaired GABAergic dendritic inhibition," *Eur. J. Neurosci.*, vol. 15, no. 9, pp. 1499–1508, May 2002.
- [9] B. H. Jansen and V. G. Rit, "Electroencephalogram and visual evoked potential generation in a mathematical model of coupled cortical columns," *Biol. Cybern.*, vol. 73, no. 4, pp. 357–366, Sep. 1995.
- [10] A. van Rotterdam, F. H. Lopes da Silva, J. van den Ende, M. A. Viergever, and A. J. Hermans, "A model of the spatial-temporal characteristics of the alpha rhythm," *Bull. Math. Biol.*, vol. 44, no. 2, pp. 283–305, Jan. 1982.
- [11] J. F. Tellez-Zenteno, R. S. McLachlan, A. Parrent, C. S. Kubu, and S. Wiebe, "Hippocampal electrical stimulation in mesial temporal lobe epilepsy," *Neurology*, vol. 66, no. 10, pp. 1490–1494, May 2006.